

Reducing dynamin 2 expression rescues X-linked Centronuclear Myopathy

Cowling et al.

SUPPLEMENTARY DATA

SUPPLEMENTARY METHODS

Materials. Primary antibodies used were: mouse anti-DHPR α_1 (Ca $_v$ 1.1) subunit (MA3–920; Affinity Bioreagents), α -actinin (EA-53, Sigma-Aldrich), caveolin-3 (clone 26, BD Biosciences), desmin (Y-20; Santa Cruz Biotechnology) and glyceraldehyde-3-phosphate dehydrogenase (GAPDH, MAB374; Chemicon) monoclonal antibodies; and rabbit anti-RYR1 (a kind gift from Isabelle Marty, Grenoble Institut des Neurosciences, France). Rabbit anti-DNM2 antibodies (R2680 and R2865, characterized in (1)) and anti-MTM1 (R2827)(2) were made onsite at IGBMC. Alexa-conjugated secondary antibodies were purchased from Invitrogen. Secondary antibodies against mouse and rabbit IgG, conjugated with horseradish peroxidase (HRP) were purchased from Jackson ImmunoResearch Laboratories. The following products were purchased: Hoechst nuclear stain (B2883, Sigma-Aldrich), ECL chemiluminescent reaction kit (Pierce), LipofectamineTM (Life Technologies), Tri reagent (Molecular Research Center, Ohio, USA), SYBR Green 1 Master kit (Roche Diagnostics), miScript reverse transcription kit (Qiagen), specific miScript primer assays (Qiagen) and an miScript Sybr green PCR kit (Qiagen). Patient control biopsies AHJ38 (1.5 months) and 39 (3.4 months), XLCNM biopsies with MTM1 mutations used were AHJ35 (15 days)(MTM1- intron 11-10A>GS420_R421insFIQ) and AHJ36 (1m) (MTM1-c.445-49_445-4del), 1 (MTM1-p.Leu213Pro) and 15 (MTM1- p.Ileu466dup)(3) and patient 12129/89 (MTM1- p.Val49PhefsX6). All patient biopsies used in this manuscript were either described elsewhere (as indicated), or were identified as part of routine diagnosis (data not shown).

Generation of *Mtm1*-/*yDnm2*^{skm+/-} and *Mtm1*-/*yDnm2*^{(f)skm+/-} mice. The creation and characterization of *Mtm1*-/*y* mice were described previously (4, 5). Human skeletal muscle α -actin (HSA-Cre) C57BL/6 and HSA Cre-ER^{T2} mice were a kind gift from Daniel Metzger, IGBMC, France (6, 7). Floxed *Dnm2*^{+/-} mice were bred with HSA-Cre mice and HSA Cre-ER^{T2} to produce Cre-positive

$Dnm2^{skm+/-}$ and $Dnm2^{skm(i)+/-}$ mice respectively. Male $Dnm2^{skm+/-}$ or $Dnm2^{(i)skm+/-}$ mice were bred with female $Mtm1+/-$ mice. Male offspring with the following genotypes were analyzed; line 1: $Mtm1+/-yDnm2+/+$ (WT), $Mtm1-/-yDnm2+/+$ ($Mtm1-/-y$), $Mtm1-/-yDnm2^{skm+/-}$; and line 2: $Mtm1+/-yDnm2+/+$ (WT), $Mtm1-/-yDnm2+/+$ ($Mtm1-/-y$), $Mtm1-/-yDnm2+/-HSA-Cre-ER^{T2}$ tamoxifen inducible ($Mtm1-/-yDnm2^{(i)skm+/-}$) mice. To induce excision of $Dnm2$ after birth, 3 week old mice were injected with 1mg of tamoxifen (concentration 1mg/100 μ l), daily for 3 days. All mice were sacrificed at 16 weeks of age. All mice analyzed were male, 50% 129pas strain ($Mtm1-/-y$) 50% C57BL/6 strain (HSA promoter) mice.

Phenotyping of $Dnm2+/-$ mice. Blood chemistry, ECG measurements, Dexascan, and Electromyography tests presented here for male mice (n=10 per group) were performed as part of pipelines 1 and 2 of the EUMODIC phenotyping program, at the Institut Clinique de la Souris (ICS, Illkirch, France, <http://www.ics-mci.fr/>)(8). A routine blood chemistry screen was performed on plasma from mice using an OLYMPUS AU-400 automated laboratory work station (Olympus France SA, Rungis, France), which measured many factors including urea, calcium, and total cholesterol (9). A Dual-energy X-ray absorptiometry scan (Dexascan) measuring body weight, body length, fat and bone mass, bone mass density and lean mass was performed as previously described (9). Surface electrocardiography (ECG) was performed using an Electrocardiogram FUDUKA FX 3010 associated with the EMKA software, which measured electrical activity of the heart in anesthetized mice. Electromyography (EMG) recordings were performed using a Key Point electromyography (EMG) apparatus (Medtronic, France). Sensory nerve conduction velocity (SNCV) was recorded at the level of the caudal nerve. Body temperature was maintained at 37°C with a homeostatic blanket (Harvard, France) throughout the duration of the test.

String, grip (2 and 4 paws), hang, rotarod and footprint tests. String test: Mice were suspended on a wire by their forelimbs, and allowed 20 seconds to climb their hindlimbs onto the wire. Three trials per mouse were performed, with 5 minutes rest between trials. A fall was considered equal to 20 seconds (n=minimum 5 mice per group). Grip strength tests: Performed by placing the 2 front paws or all 4 paws on the grid of a dynamometer (Bioseb, Chaville, France) and mice were pulled by the tail in

the opposite direction. The maximal strength exerted by the mouse before losing grip was recorded. Three trials per mouse were performed, with 30 seconds rest between trials (2 paw test, n=minimum 5 mice per group; 4 paw test, n=5-7 mice per group). Hanging test: mice were suspended from a cage lid for a maximum of 60 seconds. The time the mouse fell off the cage was recorded for each trial. Three trials per mouse were performed. Rotarod test: Coordination and whole body muscle strength and fatigability were tested using an accelerated rotating rod test (Panlab, Barcelona, Spain). Mice were placed on the rod which accelerated from 4 to 40 rpm during 5 minutes. Three trials per day, with 5 minutes rest between trials were performed for day 1 (training day) then 4 days which were recorded. Animals were scored for their latency to fall (in seconds). The mean of the three trials was calculated for each experiment listed above (n=5-7 mice per group). Footprint test: Hindfeet of mice were coated with nontoxic ink, and mice were allowed to walk through a tunnel (50 cm long, 9 cm wide, 6 cm high) with paper lining the floor. The angle between the hindlimbs was then measured from the footprint pattern generated, using ImageJ analysis program. A minimum of 6 footprints per mouse was analyzed (n=5-8 mice per group).

TA muscle contractile properties. Muscle force measurements were evaluated by measuring *in situ* muscle isometric contraction in response to nerve and muscle stimulation, as described previously (1). Results from nerve stimulation are shown (n=5-11 mice per group). Fatigue was measured as time taken to reach 50% of the maximum force produced. After contractile measurements, the animals were killed by cervical dislocation. TA muscles were then dissected and weighed to determine specific maximal force.

Diaphragm muscle contractile properties. Diaphragm isometric contraction was assessed on muscle strips from the ventral part of the costal diaphragm, as previously described (10). Two muscle strips per mouse were dissected *in situ*. Each muscle was mounted in a tissue chamber containing a Krebs-Henseleit solution. The solution was bubbled with a gas mixture of 95% O₂-5% CO₂ and maintained at 27°C and pH 7.4. Muscle extremities were held in spring clips and attached to an electromagnetic force transducer. Diaphragm strips were electrically stimulated by means of two platinum electrodes positioned parallel to the muscle and delivering electrical stimulation of 1 ms duration. Force-

frequency curve was determined. Absolute maximal force was achieved at a stimulation frequency of 100 Hz with train duration of 400 ms. At the end of the experiment, each muscle cross-sectional area (in mm²) was calculated from the ratio of muscle weight to optimal muscle length (L₀), assuming a muscle density of 1.06. Total isometric peak force was normalized per cross-sectional area to obtain total tension in mN.mm⁻² (n=3-5 mice per group).

qRT-PCR of mir-133a. miRNAs were prepared from 8w TA muscle using the miScript reverse transcription kit (Qiagen), the specific miScript primer assays (Qiagen) and an miScript Sybr green PCR kit (Qiagen) in a Lightcycler 480 (Roche) according to the recommended protocol. Results were standardized to U6 snRNA (n=4-7 mice per group). Primers used were Rn-miR-133a₂ (MS00033208, Qiagen) and Hs_RNU6B_2 (MS00014000, Qiagen).

Western blotting. Mouse muscles was minced and homogenized on ice for 3 × 30 s (Ultra Turrax homogenizer) in 10 times the weight/volume of 1% NP-40 Tris-Cl buffer, pH 8, then extracted for 30 min at 4°C. Protein concentration was determined using a DC protein assay kit (Bio-Rad Laboratories), and lysates analyzed by SDS-PAGE and western blotting on nitrocellulose membrane. Western blot films were scanned and band intensities were determined using ImageJ software (Rasband, W.S., ImageJ, U. S. National Institutes of Health, Bethesda, Maryland, USA, <http://rsb.info.nih.gov/ij/>, 1997-2009). Densitometry values were standardized to corresponding total GAPDH values and expressed as a fold difference relative to the listed control (n=5-7 mice per group).

Histological and immunofluorescence analysis of skeletal muscle. Longitudinal and transverse cryosections (8 μm) sections of mouse skeletal muscles were prepared, fixed and stained with antibodies to DHPR α_1 (1:100), RYR1 (1:200), α -actinin (1:1,000), caveolin-3 (1:1000); DNM2-R2680 (1:200), MTM1-R2827 (1:200), and desmin (1:100). Nuclei were detected by costaining with Hoechst (Sigma-Aldrich) for 10 min. Samples were viewed using a laser scanning confocal microscope (TCS SP5; Leica Microsystems, Mannheim, Germany). Air-dried transverse sections were fixed and stained with haematoxylin and eosin (HE) or succinate dehydrogenase (SDH), and image acquisition performed with a slide scanner NanoZoomer 2 HT equipped with the fluorescence module L11600-21

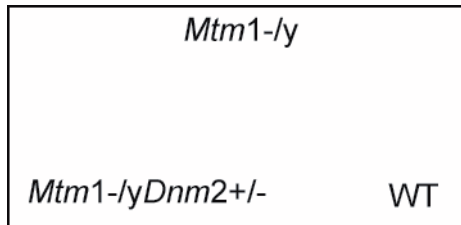
(Hamamatsu Photonics, Japan). Cross-sectional area (CSA) was analyzed in HE sections from TA mouse skeletal muscle, using FIJI image analysis software. CSA (μm^2) was calculated (>500 fibers per mouse) from 4-7 mice per group. The percentage of TA muscle fibers with centralized or internalized nuclei was counted in >500 fibers from 4-6 mice using the cell counter plugin in ImageJ image analysis software.

Transmission electron microscopy. Mice were anesthetized by intraperitoneal injection of 10 μl per body gram of ketamine (20 mg/ml, Virbac, Carros, France) and xylazine (0.4%, Rompun, Bayer, Wuppertal, Germany). TA muscle biopsies were fixed with 2.5% glutaraldehyde in 0.1 M cacodylate buffer (pH 7.2) and processed as described previously (1, 4). Triad structures were identified on longitudinal sections of muscle and the number of triads per sarcomere was quantified. The ratio of triads / sarcomere was calculated by dividing number of triads clearly identified, by the total number of sarcomeres present in the image, as described previously (11). 40-80 triads were counted per mouse.

SUPPLEMENTARY VIDEOS

Video S1. 8 week old WT, *Mtm1*^{-/y}, and *Mtm1*^{-/y}*Dnm2*^{+/-} mice in a cage.

Starting position for video 1:



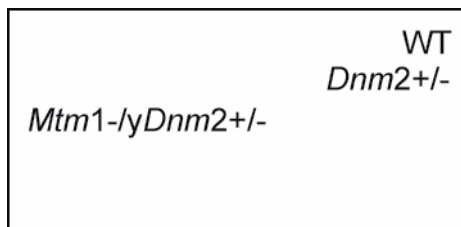
Video S2. String test on a 8 week old WT mouse

Video S3. String test on a 8 week old *Mtm1*^{-/y} mouse

Video S4. String test on a 8 week old *Mtm1*^{-/y}*Dnm2*^{+/-} mouse

Video S5. 6 month old WT, *Dnm2*^{+/-}, and *Mtm1*^{-/y}*Dnm2*^{+/-} mice in a cage

Starting position for video 5:



Video S6. Hanging test on a 8 week old WT mouse

Video S7. Hanging test on a 8 week old *Mtm1*^{-/y} mouse

Video S8. Hanging test on a 8 week old *Mtm1*^{-/y}*Dnm2*^{+/-} mouse

SUPPLEMENTARY REFERENCES

1. Cowling, B.S., Toussaint, A., Amoasii, L., Koebel, P., Ferry, A., Davignon, L., Nishino, I., Mandel, J.L., and Laporte, J. 2011. Increased expression of wild-type or a centronuclear myopathy mutant of dynamin 2 in skeletal muscle of adult mice leads to structural defects and muscle weakness. *Am J Pathol* 178:2224-2235.
2. Hnia, K., Tronchere, H., Tomczak, K.K., Amoasii, L., Schultz, P., Beggs, A.H., Payrastre, B., Mandel, J.L., and Laporte, J. 2011. Myotubularin controls desmin intermediate filament architecture and mitochondrial dynamics in human and mouse skeletal muscle. *J Clin Invest* 121:70-85.
3. Shichiji, M., Biancalana, V., Fardeau, M., Hogrel, J.Y., Osawa, M., Laporte, J., and Romero, N.B. 2013. Extensive morphological and immunohistochemical characterization in myotubular myopathy. *Brain and Behavior* In press.
4. Buj-Bello, A., Laugel, V., Messaddeq, N., Zahreddine, H., Laporte, J., Pellissier, J.F., and Mandel, J.L. 2002. The lipid phosphatase myotubularin is essential for skeletal muscle maintenance but not for myogenesis in mice. *Proc Natl Acad Sci U S A* 99:15060-15065.
5. Al-Qusairi, L., Weiss, N., Toussaint, A., Berbey, C., Messaddeq, N., Kretz, C., Sanoudou, D., Beggs, A.H., Allard, B., Mandel, J.L., et al. 2009. T-tubule disorganization and defective excitation-contraction coupling in muscle fibers lacking myotubularin lipid phosphatase. *Proc Natl Acad Sci U S A* 106:18763-18768.
6. Schuler, M., Ali, F., Metzger, E., Chambon, P., and Metzger, D. 2005. Temporally controlled targeted somatic mutagenesis in skeletal muscles of the mouse. *Genesis* 41:165-170.
7. Miniou, P., Tiziano, D., Frugier, T., Roblot, N., Le Meur, M., and Melki, J. 1999. Gene targeting restricted to mouse striated muscle lineage. *Nucleic Acids Res* 27:e27.
8. Ayadi, A., Birling, M.C., Bottomley, J., Bussell, J., Fuchs, H., Fray, M., Gailus-Durner, V., Greenaway, S., Houghton, R., Karp, N., et al. 2012. Mouse large-scale phenotyping initiatives: overview of the European Mouse Disease Clinic (EUMODIC) and of the Wellcome Trust Sanger Institute Mouse Genetics Project. *Mamm Genome* 23:600-610.

9. Gates, H., Mallon, A.M., and Brown, S.D. 2011. High-throughput mouse phenotyping. *Methods* 53:394-404.
10. Coirault, C., Lambert, F., Marchand-Adam, S., Attal, P., Chemla, D., and Lecarpentier, Y. 1999. Myosin molecular motor dysfunction in dystrophic mouse diaphragm. *Am J Physiol* 277:C1170-1176.
11. Amoasii, L., Bertazzi, D.L., Tronchere, H., Hnia, K., Chicanne, G., Rinaldi, B., Cowling, B.S., Ferry, A., Klaholz, B., Payrastre, B., et al. 2012. Phosphatase-dead myotubularin ameliorates X-linked centronuclear myopathy phenotypes in mice. *PLoS Genet* 8:e1002965.

WEBSITES

<http://www.eumodic.eu/>

<http://www.euromphenome.org/>

<http://www.ics-mci.fr/>

<http://rsb.info.nih.gov/ij/>

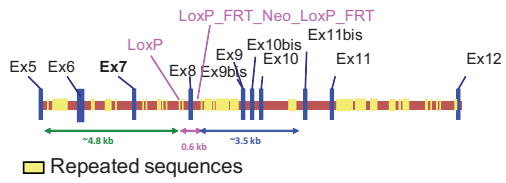


Figure S1. Targeted disruption of mouse *Dnm2* to create *Dnm2* heterozygous (*Dnm2*^{+/-}) mice. The genomic region surrounding the targeted exon 8 of *Dnm2* in mice. Deletion of exon 8 is predicted to lead to an out-of-frame transcript.

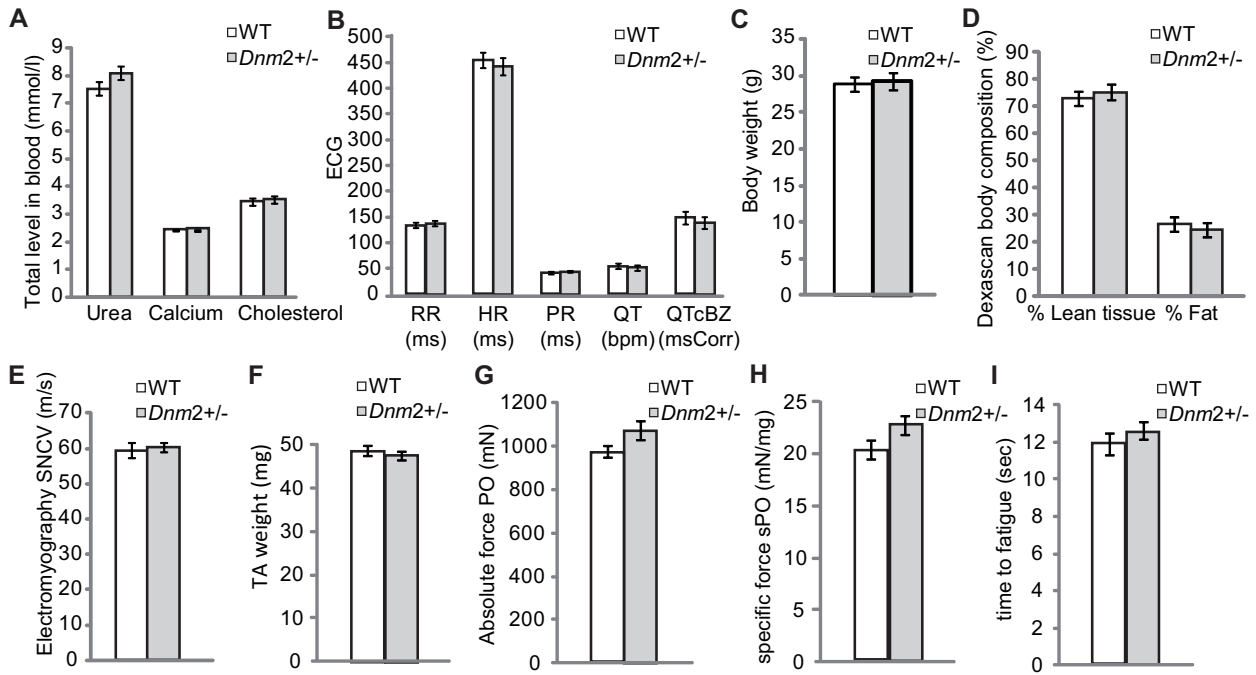


Figure S2. Biochemical and phenotypic characterization of *Dnm2* heterozygous mice. (A) Blood analysis of urea, calcium, and total cholesterol levels in *Dnm2* heterozygous (*Dnm2*^{+/-}) and wild type (WT) mice. (B) Electrocardiograph (ECG) measurements in WT and *Dnm2*^{+/-} mice. X-axis values represent measurements shown below each test as follows; RR (interval between two R waves, measured in ms); HR = heart rate (ms); PR (interval from P-R wave, ms); QT (interval from Q-T waves, bpm); QTcBZ (QT corrected, msCorr). (C) Whole body weight. (D) Dexascan for whole body composition. The amount of lean tissue and fat are shown as a percentage of total body composition. (E) Single nerve conduction velocity (SNCV) results from muscle electromyography performed on WT and *Dnm2*^{+/-} mice. (F) Total mass of the TA muscle. Absolute (G) and specific (H) maximal force of the TA muscle. (I) Measurement of fatigue of the TA muscle, fatigue represents time to 50% maximal force production in seconds (s). All mice analyzed were 10-15 week old male mice (n=8-12 per group). All graphs depict mean \pm s.e.m and none of the evaluated parameters were significantly different between WT and *Dnm2*^{+/-} mice.

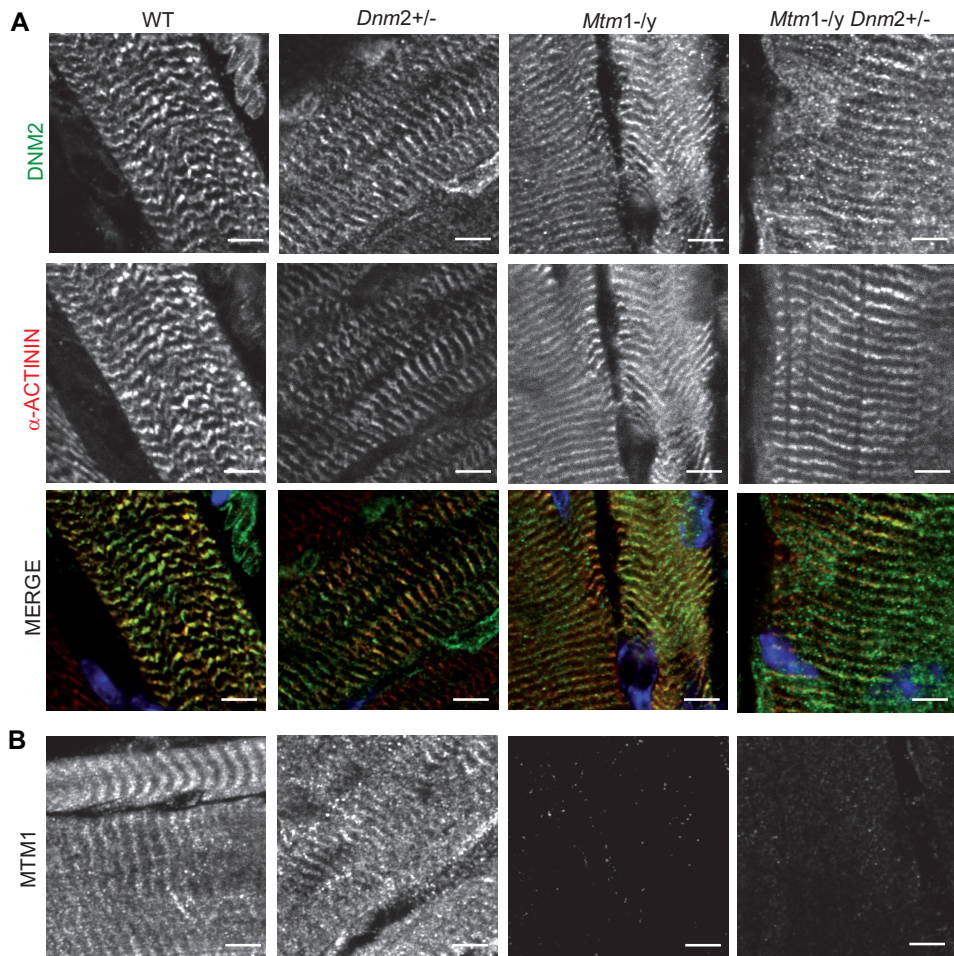


Figure S3. DNM2, MTM1, and α -actinin localization in TA muscles. Longitudinal muscle sections from 8 week old mice were co-stained with DNM2-R2680 (green) and α -actinin (red) (A) antibodies or stained with MTM1-R2827 (B) antibody and imaged by confocal microscopy. Scale bar 5 μ m.

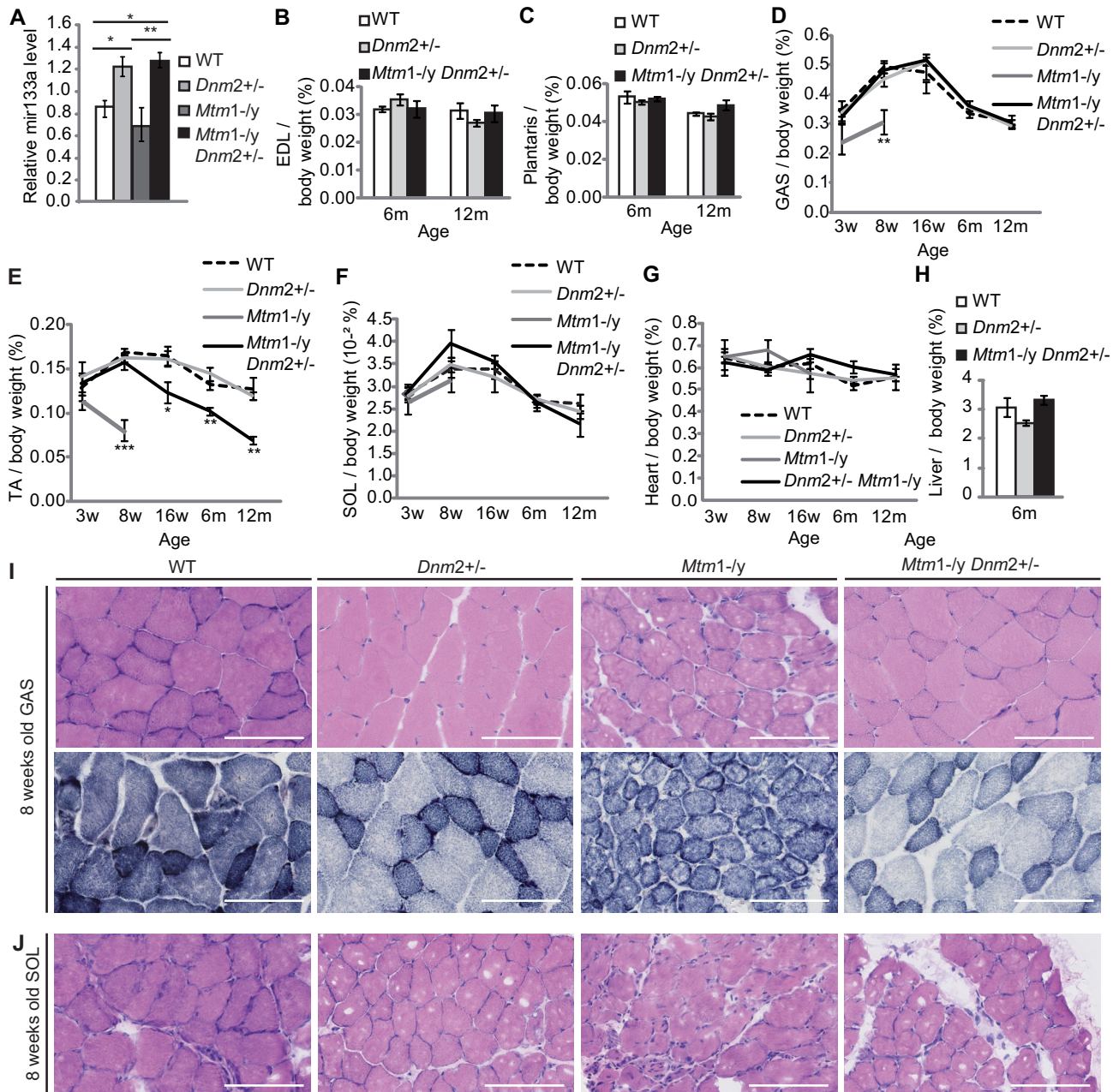


Figure S4. Atrophy is rescued in skeletal muscles of *Mtm1-ly* mice with reduced DNMT2 expression. (A) mRNA levels were quantified by qRT-PCR analysis, expressed relative to U6 loading control. $n=3$ independent experiments. EDL (B), plantaris (C), GAS (D), TA (E), SOL (F), heart (G), and liver (H) weights are reported as a percentage of total body weight ($n=5-15$ mice). All graphs depict mean \pm s.e.m. (* $p<0.05$, ** $p<0.01$, *** $p<0.001$) (w=weeks of age, m=months of age). Transverse GAS (I) or SOL (J) sections from 8 week old mice stained with HE (upper panel) or SDH (lower panel). Scale bar 100 μ m.

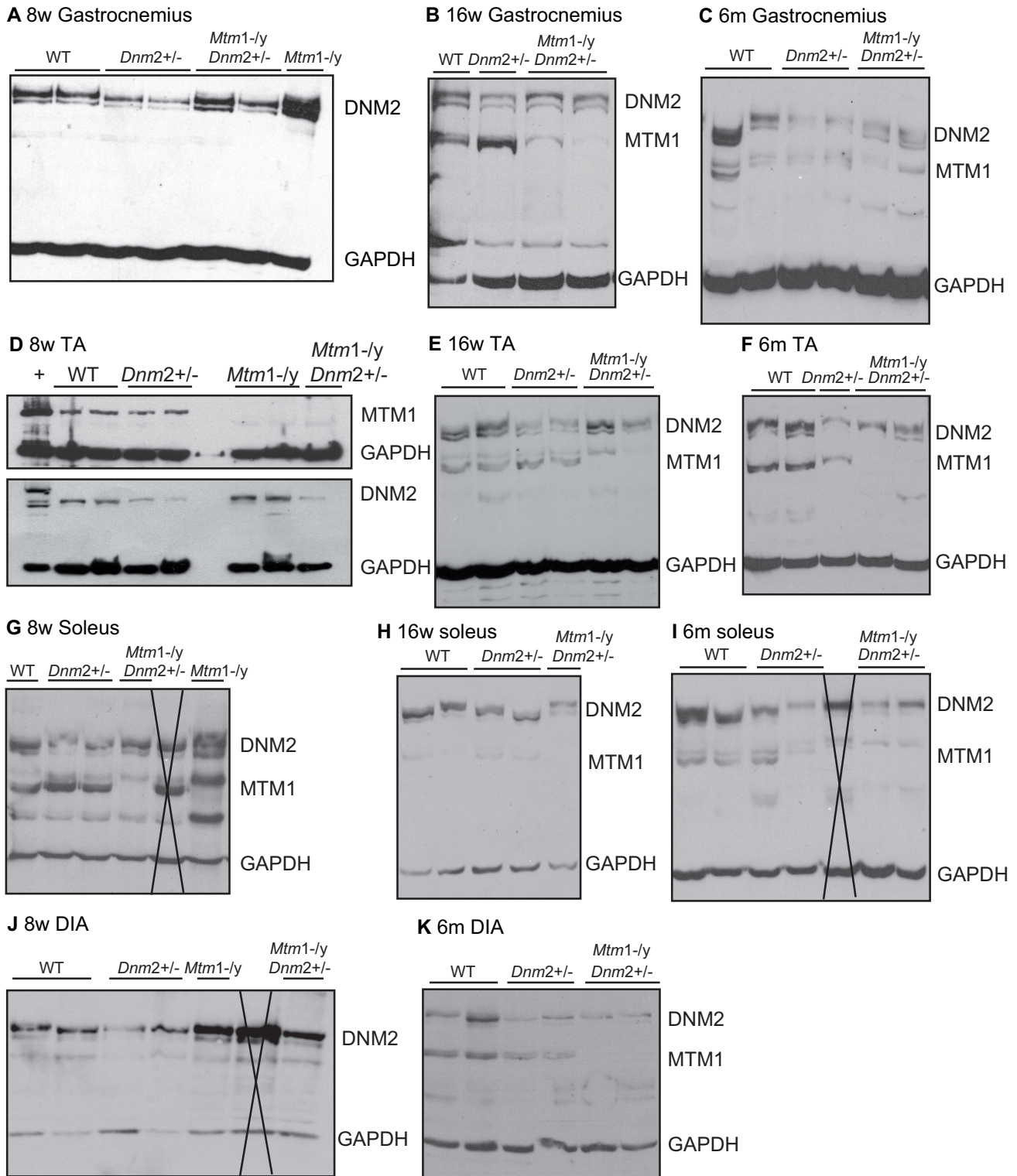


Figure S5. Original scans of western blots showing protein expression levels in various muscles at different ages. Lysates from 8 (A,D,G,J), 16 (B,E,H) weeks and 6 months (C,F,I,K) old gastrocnemius (GAS) (A-C), tibialis anterior (TA) (D-F), soleus (G-I), and diaphragm (J,K) muscles were immunoblotted for DNM2 and GAPDH (loading control). Where listed, lysates were also blotted for MTM1. When a doublet is present, MTM1 is represented by the lower band. Intervening lanes not relevant to this study were marked with a cross (G, I, J).

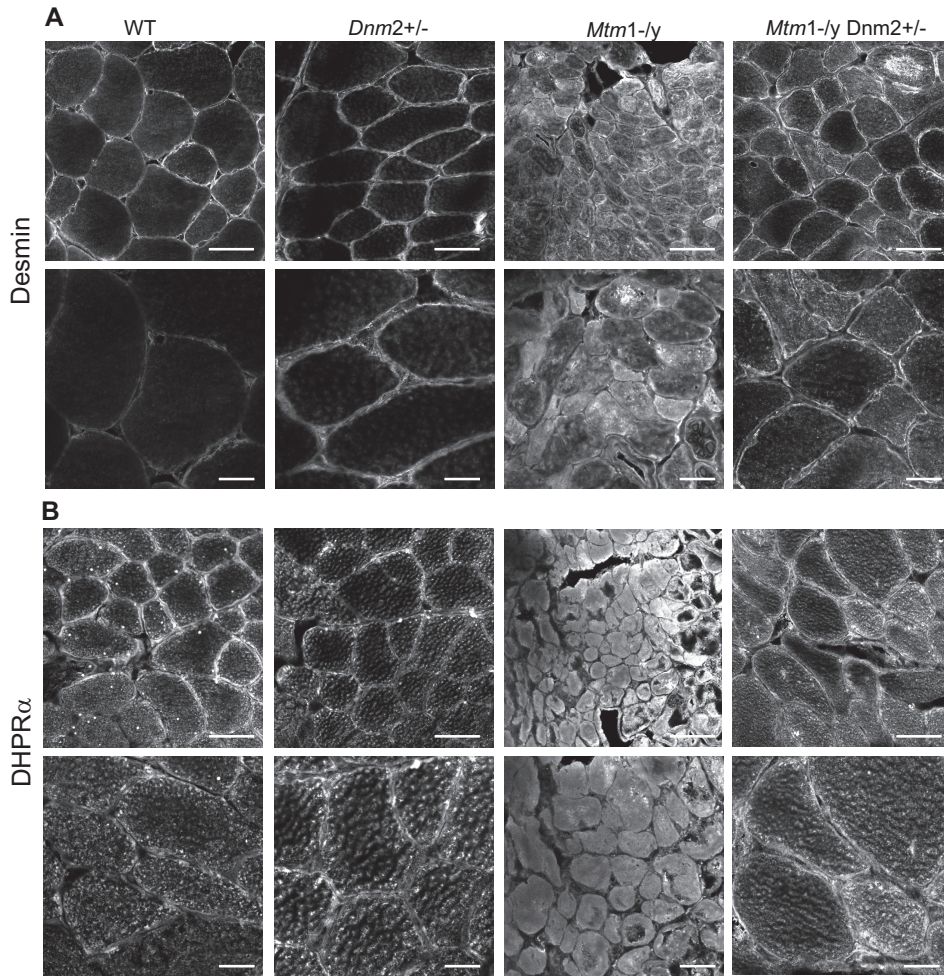
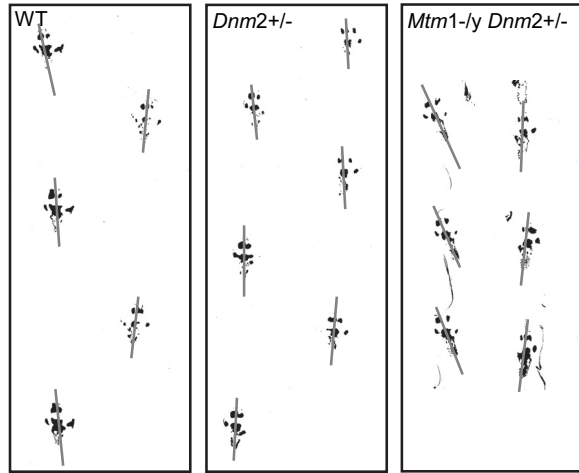
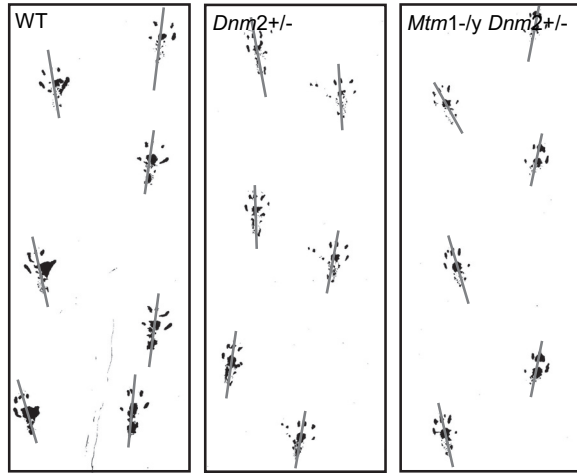


Figure S6. Localization of desmin and triad markers are rescued in TA muscles from 8 week old *Mtm1-ly* mice with reduced DNM2 expression. Transverse muscle sections from 8 week old mice were stained with a desmin (A) or DHPR α (B) antibody and imaged by confocal microscopy. Scale bar 50 μm (upper panel) and 20 μm (lower panel) for both. Note the cytosolic accumulation of desmin in *Mtm1-ly*, which is rescued in most *Mtm1-lyDnm2+/-* fibers.

A. Footprint patterns from 6 month old mice



Footprint patterns from 12 month old mice



B

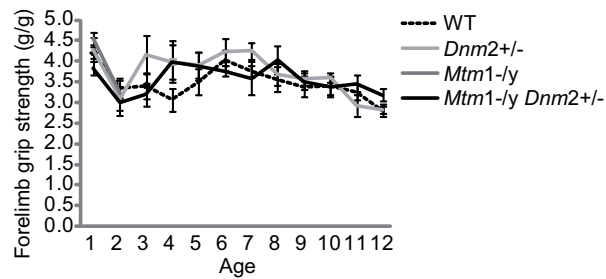


Figure S7. (A) Footprint patterns from 6 and 12 month old mice. A line of best fit is drawn to depict the angle measured between hindfeet. Notably *Mtm1*^{-ly} *Dnm2*^{+/-} walk with their feet turned out compared to WT and *Dnm2*^{+/-} mice. Analyzed data is shown in figure 7B. (B) Forelimb grip test (front paws) was performed monthly (n=minimum 5 mice per group). Graph depicts mean \pm s.e.m. No significant difference was observed between groups.

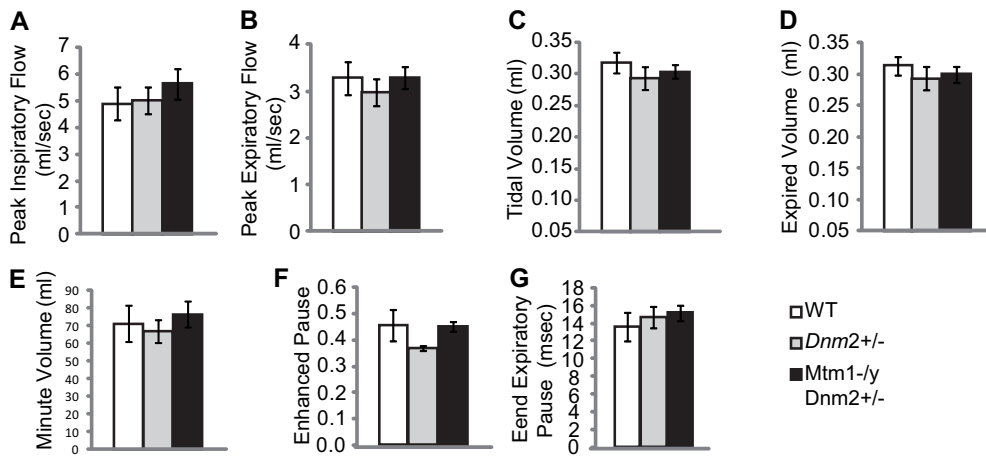


Figure S8. Plethysmograph results for 6 month old *Mtm1*^{-/-} mice with reduced DNM2 expression. The plethysmograph test was performed on resting mice to assess resting breathing patterns. All graphs depicts mean \pm s.e.m. No significant difference was observed between groups.

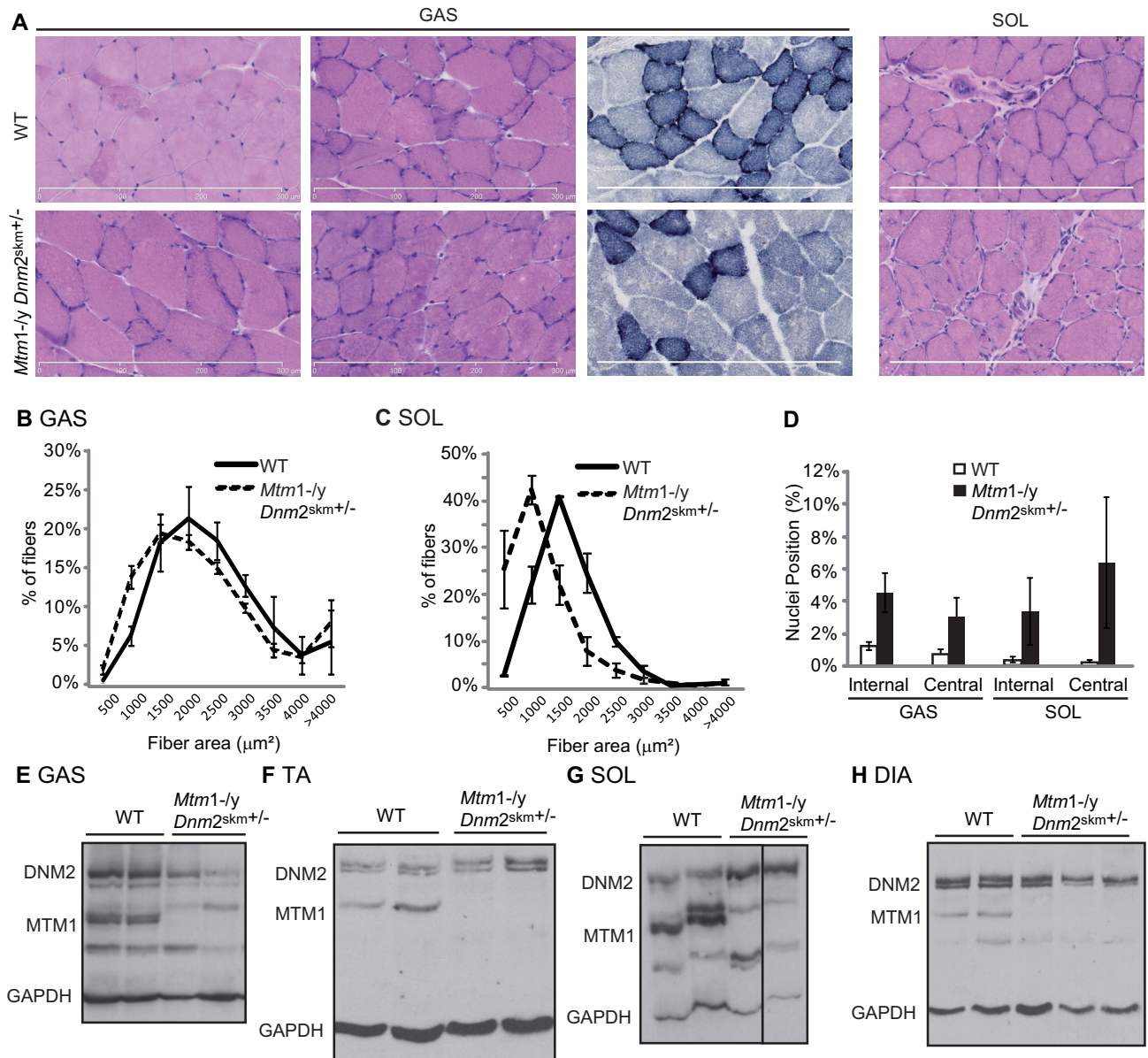


Figure S9. Heterozygous deletion of DNM2 in skeletal muscle alone ameliorates the pathology of *Mtm1-/-* mice. (A) Transverse TA sections from 16 week old mice were stained with HE or SDH. Scale bar 300 μm . Transverse sections from 16 week old GAS (B) and SOL (C) muscles analyzed for fiber area. Fiber size is grouped into 500 μm^2 intervals, and represented as a percentage of total fibers in each group (n=3-6 mice). (D) The frequency of fibers with internal or central nuclei were counted (n=3-6 mice). Gastrocnemius (GAS)(E), tibialis anterior (TA) (F), soleus (SOL)(G, images shown are from the same western blot) and diaphragm (H) muscle lysates from 16 week old mice were immunoblotted for DNM2, MTM1 and GAPDH (loading control). All graphs depict mean + s.e.m. (*p<0.05, **p<0.01, ***p<0.001).

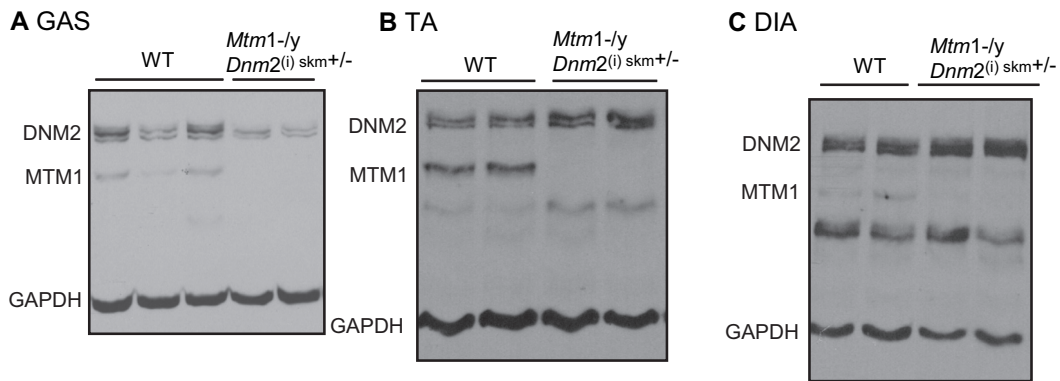


Figure S10. Protein expression levels in *Mtm1-lyDnm2skm+/-* mice. Gastrocnemius (GAS)(A), tibialis anterior (TA) (B), and diaphragm (C) skeletal muscle lysates from 16 week old mice were immunoblotted for DNM2, MTM1 and GAPDH (loading control).